5154 *Biochemistry* **2010,** *49,* 5154–5159
DOI: 10.1021/bi902172n

BIOCHEMISTRY
including biophysical chemistry & molecular biology
Article

Characterization of Chloride-Depleted Human Sulfite Oxidase by Electron Paramagnetic Resonance Spectroscopy: Experimental Evidence for the Role of Anions in Product Release[†]

Asha Rajapakshe, Kayunta Johnson-Winters, Anna R. Nordstrom, Kimberly T. Meyers, Safia Emesh, Andrei V. Astashkin,* and John H. Enemark*

Department of Chemistry and Biochemistry, University of Arizona, Tucson, Arizona 85721

Received December 17, 2009; Revised Manuscript Received May 19, 2010

ABSTRACT: The Mo(V) state of the molybdoenzyme sulfite oxidase (SO) is paramagnetic and can be studied by electron paramagnetic resonance (EPR) spectroscopy. Vertebrate SO at pH <7 and >9 exhibits characteristic EPR spectra that correspond to two structurally different forms of the Mo(V) active center termed the low-pH (*lpH*) and high-pH (*hpH*) forms, respectively. Both EPR forms have an exchangeable equatorial OH ligand, but its orientation in the two forms is different. It has been hypothesized that the formation of the *lpH* species is dependent on the presence of chloride. In this work, we have prepared and purified samples of the wild type and various mutants of human SO that are depleted of chloride. These samples do not exhibit the typical *lpH* EPR spectrum at low pH but rather exhibit spectra that are characteristic of the *blocked* species that contains an exchangeable equatorial sulfate ligand. Addition of chloride to these samples results in the disappearance of the *blocked* species and the formation of the *lpH* species. Similarly, if chloride is added before sulfite, the *lpH* species is formed instead of the *blocked* one. Qualitatively similar results were observed for samples of sulfite-oxidizing enzymes from other organisms that were previously reported to form a *blocked* species at low pH. However, the depletion of chloride has no effect upon the formation of the *hpH* species.

The sulfite-oxidizing enzymes (SOEs),[1] represented by sulfite oxidase (SO) in vertebrates and plants and sulfite dehydrogenase (SDH) in bacteria, catalyze the oxidation of sulfite to sulfate as given by generic eq 1 (*1*).

$$SO_3^{2-} + H_2O \rightarrow SO_4^{2-} + 2H^+ + 2e^- \quad (1)$$

In humans, SO is essential for normal neonatal neurological development, and inborn deficiencies in SO result in severe physical and neurological disorders and early death (*2*, *3*).

Reaction 1 is catalyzed by the square-pyramidal oxo-molybdenum active center, which has three equatorial sulfur ligands (one from the conserved cysteinyl side chain and two from the molybdopterin cofactor), one axial oxo ligand, and an exchangeable equatorial oxo ligand in the solvent accessible pocket of the active site (*4*, *5*). During the proposed catalytic cycle (*6*), sulfite initially reduces Mo(VI) to Mo(IV). Regeneration of the Mo(VI) state involves two one-electron oxidations, as shown in Scheme 1 (only the exchangeable equatorial ligand of the Mo ion is shown). The intermediate Mo(V) state is paramagnetic and has been extensively studied by electron paramagnetic resonance (EPR) spectroscopy (*7*−*14*).

Unlike X-ray crystallography or extended X-ray absorption fine structure (EXAFS) spectroscopy, EPR spectroscopy can detect protons in the vicinity of a paramagnetic center and is able to unequivocally identify specific nuclei through using substitutions by or permutations of magnetic isotopes (e.g., $^{16}O \rightarrow {}^{17}O$, $^{35}Cl \rightarrow {}^{37}Cl$, $^{14}N \rightarrow {}^{15}N$, etc.). Both continuous wave (CW) and pulsed EPR spectroscopic approaches have been used to establish the effects of pH, anions in the media, and mutations near the active site on the identity and structure of the exchangeable equatorial ligand of the Mo(V) ion. It was found that in the absence of inhibiting anions (e.g., PO_4^{3-} and AsO_4^{3-}), wild type (*wt*) vertebrate SO can show two distinct types of EPR signals, high-pH (*hpH*) and low-pH (*lpH*), corresponding to two different structural forms of the Mo active center. For both of these forms, the exchangeable equatorial ligand is OH (see stage 3 of Scheme 1). However, in some mutant forms of vertebrate SO (Y343F, R160Q hSO), as well as in the R55Q variant of bacterial SDH, and *wt* plant SO (At-SO from *Arabidopsis thaliana*), two types of low-pH *blocked* forms have recently been observed, in which the exchangeable equatorial ligand is sulfate (bound product) rather than OH (stage 3A of Scheme 1) (*15*−*17*). The lethality of the pathogenic R160Q mutation in hSO has been attributed to the occurrence of the *blocked* form (*16*), which may represent a catalytic dead end, and inefficient intramolecular electron transfer (*18*).

[†]This research was supported by National Institutes of Health (NIH) Grant GM-037773 (to J.H.E.) and Ruth L. Kirchstein-NIH Fellowship 1F32GM082136-01 (to K.J.-W.). The construction of the pulsed EPR spectrometers was supported by grants from the National Science Foundation (DBI-0139459, DBI-9604939, and BIR-9224431) and the NIH (S10RR020959) for development of the pulsed EPR facility. K.T. M. is a participant in the Undergraduate Biology Research Program, supported in part by a grant to the University of Arizona from the Howard Hughes Medical Institute (52005889).

*To whom correspondence should be addressed. A.V.A.: phone, (520) 621-9968; fax, (520) 626-8065; e-mail, andrei@u.arizona.edu. J. H.E.: phone, (520) 621-2245; fax, (520) 626-8065; e-mail, jenemark@u.arizona.edu.

[1]Abbreviations: SO, sulfite oxidase; SOEs, sulfite-oxidizing enzymes; SDH, sulfite dehydrogenase; EPR, electron paramagnetic resonance; *lpH*, low-pH; *hpH*, high-pH; DFT, density functional theory; ESEEM, electron spin-echo envelope modulation; HYSCORE, hypefine sublevel correlation; *hfi*, hyperfine interaction; *wt*, wild type; *nqi*, nuclear quadrupole interaction.

 Published on Web 05/21/2010

Scheme 1: Simplified Catalytic Cycle of SO and SDH[a]

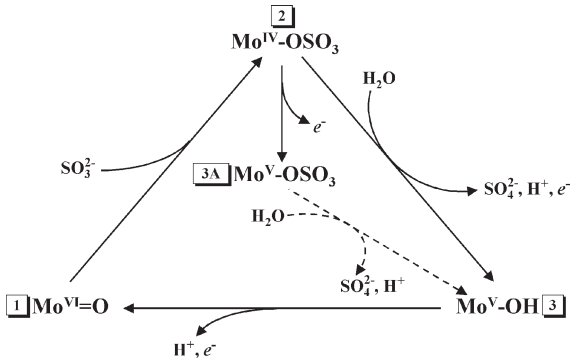

[a]Stage 1 corresponds to the resting state of the enzyme. The 1 → 2 → 3 → 1 pathway corresponds to the normal catalytic turnover. Depending on the buffer pH, stage 3 corresponds to the *hpH* or *lpH* form of the active center. Stage 3A (typically observed at a low pH of < 7) corresponds to the *blocked* form of the active center. In *wt* vertebrate SO, stage 3A is generated in chloride-depleted samples at low pH. Addition of chloride results in hydrolysis of sulfate (3A → 3 transition).

Previous pH titrations of vertebrate SO have shown that the equilibrium between the *lpH* and *hpH* forms depends on the amount of Cl^- added to the buffer in the form of NaCl (*12*). From these experiments, it was hypothesized that Cl^- is an integral part of the *lpH* form, likely to be coordinated to the Mo ion. Attempts to detect the hyperfine interaction (*hfi*) with this chloride were later undertaken by Doonan et al. using CW EPR and ^{35}Cl- or ^{37}Cl-enriched NaCl (*19*). While some differences between the ^{37}Cl- and ^{35}Cl-enriched samples were observed, they were at the limit of experimental accuracy. The weakness of the experimental CW EPR evidence for chloride interaction was, however, alleviated by the fact that when fluoride, bromide, or iodide was used instead of chloride, clearly observable EPR splittings due to the halogen nucleus *hfi* were detected (*12*, *19*). On the basis of these data, the chloride ligand was suggested to be weakly coordinated at the axial position of the Mo(V) center *trans* to the axial oxo ligand (*19*).

More conclusive and detailed information about the interaction between Mo and Cl in *lpH* SO was obtained recently using pulsed EPR and DFT calculations (*17*). The electron spin-echo envelope modulation (ESEEM) caused by ^{35}Cl and ^{37}Cl was unequivocally detected, and the *hfi* and nuclear quadrupole interaction (*nqi*) parameters of the nearby chlorine nucleus were determined. DFT calculations performed for various structural models for incorporation of Cl^- into the active site established that Cl^- does not coordinate in the axial position but rather is hydrogen bonded to the equatorial OH ligand, to the hydrogen atoms of the surrounding OH groups, and to amino acid residues of the binding site. Interestingly, even a sample of hSO purified elsewhere and prepared without added chloride exhibited a CW EPR spectrum characteristic of the *lpH* form (*12*, *19*), as well as a $^{35,37}Cl$ ESEEM (*17*). Thus, it was hypothesized that Cl^- may be essential for the formation of the *lpH* form, and that *wt* vertebrate SO has a high affinity for Cl^- at low pH (*17*).

Here we report that an SOE apparently lacking chloride near the Mo active site can be prepared when the enzyme is purified using an initial desalting column approximately twice as large as that employed in earlier preparations (*20*, *21*). The *wt* hSO purified in this manner does not exhibit the typical *lpH* species at pH ~6 but shows instead formation of the *blocked* species, as confirmed by detection of characteristic ^{33}S ESEEM in a sample prepared with ^{33}S-labeled sulfite. A similar result was also obtained for various mutated hSO enzymes. Addition of chloride to these samples converted their EPR spectra to that of the typical *lpH* form (transition between stages 3A and 3 in Scheme 1) with the exception of the lethal R160Q mutant of hSO. Similarly, adding chloride before the reduction with sulfite resulted in the formation of the *lpH* species instead of the *blocked* one.

MATERIALS AND METHODS

Recombinant *wt* hSO and mutant forms of hSO were expressed and purified as previously described (*20*, *21*). The chloride content of the enzyme samples was analyzed using the QuantiChrom Chloride assay kit (DICL-250) from BioAssay Systems. Steady-state kinetic measurements were performed using the sulfite/cytochrome *c* assay reaction for SO and monitoring the reduction of cytochrome *c* at 550 nm. Concentrations of chloride and sulfite were varied, and plots of 1/rate versus 1/substrate were made for a series of chloride concentrations. The binding constant for chloride was determined from the *x* intercept of a replot of the slopes of the lines (1/rate vs 1/substrate) versus chloride concentration (see the Supporting Information).

The EPR samples at pH 5.8 were prepared in 100 mM Bis-Tris buffer. The samples at pH 7 and 9 were prepared in 100 mM Bis-Tris propane buffer. The enzyme was reduced with a 20-fold excess of sodium sulfite under argon and immediately frozen in liquid nitrogen. The same buffer system and procedure were used for reduction with ^{33}S-labeled sulfite, prepared as previously described (*15*). After the *blocked* form was detected by EPR measurements of the samples at low pH, the samples were thawed at 0 °C, 10 or 100 mM NaCl was added, the samples were frozen again, and the EPR measurements were repeated. In a parallel set of experiments, 100 mM NaCl was added to chloride-depleted enzymes prior to addition of $Na(SO_3)_2$.

The X-band (~9 GHz) CW EPR experiments were performed on a Bruker ESP300 spectrometer at 77 K. The ESEEM measurements were taken on a home-built K_a-band (26−40 GHz) pulsed EPR spectrometer (*22*). The measurement temperature was ~21 K.

The concentrations of Mo(V) in the SO enzyme samples were determined via comparison of the double integrals of the X-band CW EPR spectra recorded at 77 K with that of 5 mM $Cu(NO_3)_2$ in a glassy water/glycerol solution. For double intergation, only the well-defined EPR features of the active centers containing nonmagnetic (I = 0, with a natural abundance of ~75%) molybdenum isotopes were used. The broad and rather featureless EPR lines of the Mo(V) centers containing magnetic molybdenum isotopes (^{95}Mo and ^{97}Mo, $I = {}^5/_2$ for both, with a total natural abundance of ~25%) were suppressed by the baseline subtraction preceding the double integration. Therefore, to account for the magnetic isotopes and obtain the total concentration of the Mo(V) active centers, the estimated concentration of the centers with nonmagnetic isotopes was multiplied by $^4/_3$. Typical total concentrations of Mo(V) centers relative to the enzyme concentrations were ~40−50%. Thawing the samples to add NaCl (overall handling time at 0 °C of ~2 min) resulted in a decrease in the Mo(V) concentration to ~30−40%.

RESULTS AND DISCUSSION

Numerous previous EPR experiments with *wt* vertebrate SO at low pH (< 7) performed by us and others (*7*−*10*, *12*, *17*, *19*) always showed formation of the *lpH* EPR-active Mo(V) species

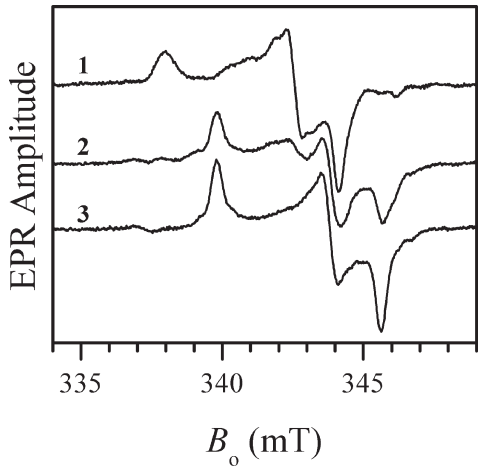

FIGURE 1: Traces 1−3 are X-band CW EPR spectra of *wt* hSO at pH 5.8, 7.0, and 9.0, respectively. No NaCl was added to the samples. Experimental conditions: microwave (mw) frequency, 9.455 GHz; mw power, 2 mW; magnetic field modulation amplitude, 0.1 mT; temperature, 77 K; enzyme concentrations, 430, 570, and 500 μM for traces 1−3, respectively. Estimated relative concentrations of Mo(V) centers were 51, 47, and 48% for traces 1−3, respectively.

with characteristic hyperfine coupling from an exchangeable proton. Recently, we began preparing and purifying recombinant *wt* hSO in our own laboratory and were initially surprised to find that the EPR signal we systematically obtained at low pH (typically, 5.8) was similar to that characteristic of the *blocked* form of SO (trace 1 in Figure 1) with coordinated sulfate (product). Similar to the *blocked* forms observed earlier in *wt* At-SO (*15*) and Y343F hSO (*16*), this EPR signal is characterized by the principal g values (g_1, g_2, and $g_3 \approx 1.999$, 1.972, and 1.963, respectively) and does not show any hyperfine splittings because the exchangeable equatorial ligand, sulfate, does not have any magnetic nuclei (the natural abundance of ^{16}O is 99.757%, and that of ^{32}S and ^{34}S is 99.2%).

To verify that the EPR signal we detected for *wt* hSO indeed belongs to the *blocked* form, the enzyme was reduced with ^{33}S-enriched sulfite, and K_a-band ESEEM experiments similar to those described elsewhere were performed (*15*, *16*). The ESEEM spectra (see Figure 2) confirm that the observed EPR signal belongs to the *blocked* form of SO. The ^{33}S *hfi* constant ($a_{iso} \approx$ 2.6 MHz) and quadrupole coupling constant ($e^2Qq/h \approx 36$ MHz) estimated from hypefine sublevel correlation (HYSCORE) spectra (see the Supporting Information) are similar to those found for the *blocked* species in other SOEs (*15*, *16*). The samples prepared at high pH (~9.0) show the formation of the usual *hpH* species (trace 3 in Figure 1) characterized by the principal g values (g_1, g_2, and $g_3 \approx 1.987$, 1.964, and 1.953, respectively) (*10*). At intermediate pH (e.g., pH 7) a mixture of the *blocked* and *hpH* forms was observed (trace 2 in Figure 1). The typical *lpH* form was not generated at any pH within the studied range from 5.8 to 9.

Careful examination of the enzyme purification and sample preparation procedures has revealed that the only difference between the published procedure (*20*, *21*) and our current procedure is in the larger size of the G25 desalting column (bed volume of 500 mL vs 250 mL) used in our initial chromatographic purification step. Taking into account the recent suggestion that Cl^- may be indispensable for the formation of the *lpH* species (*17*), we hypothesized that our EPR results can be explained if we assume that our purification procedure sufficiently reduces the Cl^-

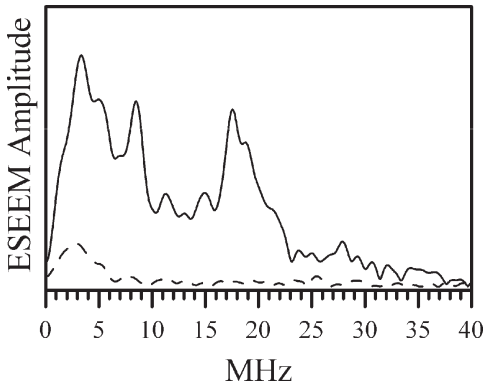

FIGURE 2: Amplitude Fourier transform spectra of normalized two-pulse ESEEM of ^{33}S-labeled [i.e., reduced with ^{33}S-enriched sulfite (—)] and unlabeled (− − −) chloride-depleted *wt* hSO at pH 5.8 obtained at the g_Y EPR turning point. Experimental conditions: mw frequency, 29.51 GHz; B_o = 1074.1 mT; mw pulses, 9 and 15 ns; temperature, 21 K; enzyme concentrations, 600 μM for trace 1 and 430 μM for trace 2. Since the only difference between the samples was in the enrichment with the magnetic isotope of sulfur (^{33}S, natural abundance of 0.76%), the lines observed in the spectrum shown by the solid line are attributed to ^{33}S.

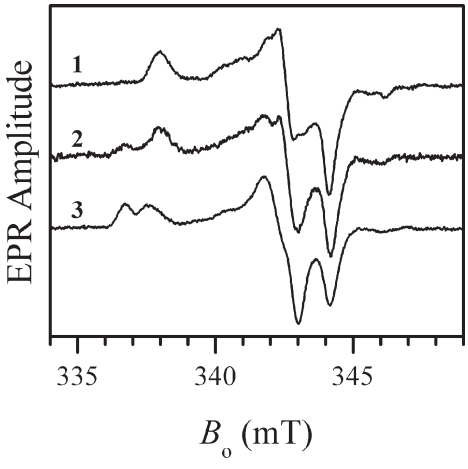

FIGURE 3: X-Band CW EPR spectra of *wt* hSO at pH 5.8 without NaCl (trace 1, same as trace 1 in Figure 1), with 10 mM NaCl (trace 2), and with 100 mM NaCl (trace 3). Experimental conditions: mw frequency, 9.455 GHz; mw power, 2 mW; magnetic field modulation amplitude, 0.1 mT; temperature, 77 K; enzyme concentrations, 430 μM for traces 1 and 3 and 270 μM for trace 2. Estimated relative concentrations of Mo(V) centers were 51, 30, and 40% for traces 1−3, respectively.

concentration to preclude formation of the usual *lpH* form of SO. Indeed, the measurement of the chloride content of our enzyme samples prepared for EPR studies at pH 5.8 yielded a $[Cl^-]/[SO]$ ratio of ~20. For comparison, the chloride concentration in samples of hSO purified elsewhere with the smaller desalting column was significantly larger ($[Cl^-]/[SO] \approx 30-40$).

To test if this low chloride concentration was responsible for the formation of the *blocked* species instead of the *lpH* form, Cl^- was added to the low-pH sample of *wt* hSO that was purified in our laboratory as described above. Adding 10 mM NaCl resulted in the formation of a substantial amount of the *lpH* species [characterized by the principal g values (g_1, g_2, and $g_3 \approx 2.004$, 1.973, and 1.966, respectively)] showing the hyperfine splittings (A_1, A_2, and $A_3 \approx 0.8$, 0.8, and 1.3 mT, respectively) at the EPR turning points caused by the *hfi* with the OH ligand proton (*10*), and a significant decrease in the amount of the *blocked* form

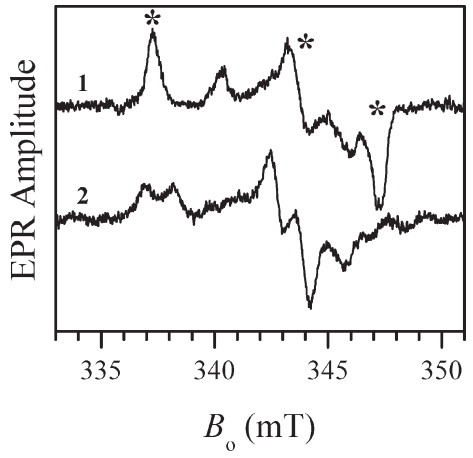

FIGURE 4: X-Band CW EPR spectra of R55Q SDH at pH 4.9 without added NaCl (trace 1) and with 100 mM NaCl (trace 2). Experimental conditions: mw frequency, 9.470 GHz; mw power, 2 mW; magnetic field modulation amplitude, 0.1 mT; temperature, 77 K; enzyme concentration, 300 μM. The asterisks over trace 1 show the EPR turning points of the *blocked* species. The minor features in trace 1 belong to the *hpH* form. Estimated relative concentrations of Mo(V) centers were 42 and 30% for traces 1 and 2, respectively.

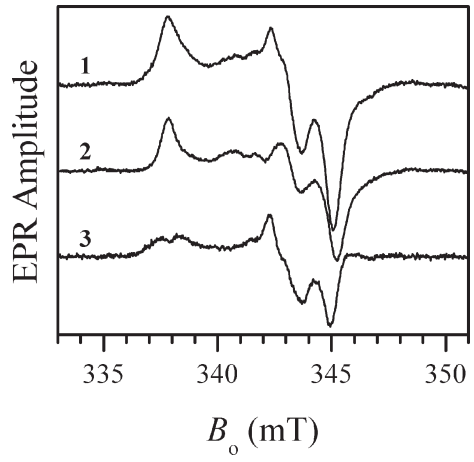

FIGURE 5: X-Band CW EPR spectra of *wt* At-SO at pH 6.0 with added 100 mM NaCl (trace 1) and without NaCl (trace 2). Trace 3 represents the difference between traces 1 and 2 showing the contribution of the *lpH* SO spectrum obtained after addition of chloride. Experimental conditions: mw frequency, 9.483 GHz; mw power, 2 mW; magnetic field modulation amplitude, 0.1 mT; temperature, 77 K; enzyme concentration, 460 μM. Estimated relative concentrations of Mo(V) centers were 35 and 42% for traces 1 and 2, respectively.

(compare traces 1 and 2 in Figure 3). An EPR sample with 100 mM NaCl gave entirely the typical *lpH* form (trace 3 in Figure 3). When 100 mM NaCl was added to an EPR sample before the reduction by sulfite, the same end result was obtained: the usual *lpH* species was generated instead of the *blocked* one.

The effect of added Cl^- on various preparations of SO and SDH that exhibited the *blocked* form was also studied for the purpose of comparison and generalization. With one exception, all of the hSO mutants purified in our lab (see the Supporting Information) that exhibited the *blocked* form when prepared at low pH without added chloride were completely converted to the typical *lpH* form via addition of 100 mM NaCl (as exemplified in Figure 3 for *wt* hSO). The exception is the pathogenic R160Q mutant (*16*), which was not affected by added Cl^- (up to 300 mM NaCl) and remained in the *blocked* form. On the other hand, for the analogous mutation (R55Q) of bacterial SDH (*23*), the *blocked* form was converted to the *lpH* form via addition of 100 mM NaCl (see Figure 4). For At-SO and Y343F hSO at pH 6, addition of 100 mM NaCl resulted in the formation of measurable amounts of the typical *lpH* species, although the EPR spectra were still dominated by the *blocked* form (as an example, see Figure 5 for the results obtained for At-SO).

The formation of the *blocked* form of hSO in chloride-depleted samples is consistent with the earlier proposal that multiple mechanisms may be possible for SO (*24*). The *blocked* form results from one-electron oxidation of the molybdenum center prior to product release to give a Mo(V)$-OSO_3$ moiety (2 → 3a transition of Scheme 1). However, the weakly coordinating sulfate ion is readily replaced in the presence of other anions at low pH. Addition of chloride gives the well-known *lpH* form (3 in Scheme 1); other halogens (F^-, Br^-, and I^-) produce the same effect (*12*, *19*). For those anions, however, the EPR splittings due to the halogen nucleus *hfi* are directly observed by CW EPR because the *hfi* constants of ^{19}F, ^{79}Br, and ^{127}I per unit of unpaired electron spin density are severalfold greater than that of ^{35}Cl and ^{37}Cl (*25*). Distinct EPR forms with coordinated phosphate (*11*, *26*) and arsenate (*9*) have also been observed at low pH. It has also been suggested that the *blocked* form actually

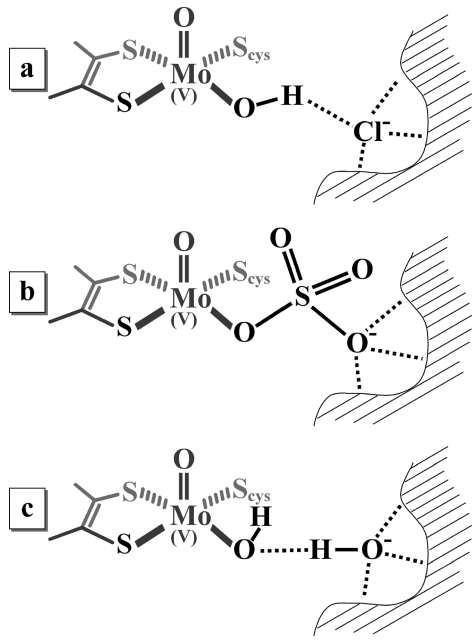

FIGURE 6: Putative structures of the substrate-accessible side of the Mo active center in (a) *lpH*, (b) *blocked*, and (c) *hpH* forms.

contains bound sulfite, the reactant, which is present in a large excess in the EPR samples (*27*, *28*).

Recently, we used $^{35,37}Cl$ ESEEM spectroscopy and DFT calculations to obtain information about the chloride binding site in the vicinity of the molybdenum active center (*17*). In contrast to earlier suggestions (*19*) that Cl^- may be coordinated in the axial position to Mo(V), *trans* to the oxo ligand, our data have shown that in *lpH* SOEs Cl^- is most likely hydrogen-bonded to the proton of the equatorial OH ligand as shown in Figure 6a. Other details of the Cl^- binding site are less definitive, although it is clear the Cl^- is stabilized in place by several hydrogen bonds, and the overall environment is fairly spherical. This is suggested by a relatively weak nuclear quadrupole interaction of this chloride ion. On the basis of X-ray structures [Protein Data Bank

Table 1: Steady-State Data for *wt* hSO with Various Amounts of NaCl Added

pH	concentration of added chloride (mM)	k_{cat} (s^{-1})	K_M(sulfite) (μM)	Cl^- dissociation constant (mM)
5.8	0	23 ± 2	2 ± 1	13 ± 3
	2.5	26 ± 1	4 ± 1	
	5	28 ± 3	6 ± 1	
	15	15 ± 1	6 ± 1	
	30	17 ± 1	5 ± 1	
	100	4 ± 1	4 ± 1	
8.0	0	27 ± 2	9 ± 3	14 ± 3
	2.5	25 ± 1	9 ± 2	
	5	25 ± 1	7 ± 1	
	10	18 ± 1	8 ± 1	
	30	15 ± 1	8 ± 1	
	100	19 ± 1	12 ± 1	

(PDB) entry 2A99 (*4*)], one of the amino acid residues involved in the Cl^- binding site in chicken SO (cSO) was thought to be W204, which corresponds to W226 in hSO. However, mutation of W226 to Ala or Phe did not affect the formation of the typical *lpH* form with added 100 mM NaCl at low pH. Therefore, the role of W226 in the stabilization of Cl^- in the enzyme in solution is questionable.

One possible qualitative explanation of the effect of chloride on the hydrolysis of sulfate from the Mo active center is that Cl^- competes with one of the distal oxygens of SO_4^{2-} for the same binding site (see Figure 6b), so that when Cl^- displaces this oxygen, SO_4^{2-} is hydrolyzed more easily. This model is indirectly supported by the fact that neither the *blocked* species detected in this work nor those studied earlier (*15*, *16*) exhibit ^{35,37}Cl ESEEM spectra.

At high pH, the hydrolysis of sulfate and the complete catalytic turnover occur in the absence of halogens, with the Mo(V) *hpH* species being formed at stage 3 of Scheme 1. The results of recent ^{1}H and ^{17}O ESEEM measurements suggest that in this case the exchangeable equatorial OH ligand is hydrogen-bonded to a second-sphere OH^- (*29*, *30*). We hypothesize, therefore, that at high pH the OH^- anion plays the same role in facilitating the hydrolysis of sulfate as the halogen anions do at low pH. The provisional structure for an *hpH* SOE based on this hypothesis is shown in Figure 6c.

It would be tempting to interpret the EPR results described above as suggesting that chloride plays a physiological role in SO by facilitating the hydrolysis of the product from the molybdenum active center. The EPR experiments, however, do not represent sufficient grounds for such an interpretation because the processes in the EPR samples of SO are limited by a single electron transfer event, and the catalytic cycle is incomplete. To assess the effects of chloride ion concentration on the overall catalytic cycle, we have conducted steady-state activity measurements on *wt* hSO at pH 5.8 and 8.0 (Table 1). At low pH (5.8), high concentrations of chloride greatly decrease the catalytic activity of recombinant hSO and exhibit "mixed" type inhibition. This result is in agreement with previous studies of the effect of chloride on the activity of native chicken SO (*31*). In addition, the presence of high concentrations of chloride (and other small anions) has an inhibitory effect on the rate constant for intramolecular electron transfer (IET) between the Mo(VI)/Fe(II) and Mo(V)/Fe(III) forms of SO (*32*). It has been proposed that small anions that can fit into the Mo active site will weaken the electrostatic attraction between the Mo and heme domains and disfavor IET. The dissociation constant for dissociation of Cl^- from hSO, measured under steady-state conditions using the sulfite/cytochrome *c* assay reaction at pH 5.8, was 13 ± 3 mM (Table 1). From this result, it follows that the chloride concentration in the EPR sample of trace 1 of Figure 1 (~5 mM) is insufficient to produce the *lpH* EPR signal. Hence, we observe the *blocked* form. The subsequent addition of chloride results in sufficient population of Cl in the active site for observation of the *lpH* signal (traces 2 and 3 of Figure 1).

At high pH (8.0), the activity decreases by ~30% as the chloride concentration is increased to 100 mM, substantially less than the 7-fold decrease at pH 5.8. The steady-state results at high pH are consistent with the fact that these samples do not exhibit ^{35,37}Cl ESEEM spectra (*15*, *16*) and give a typical *hpH* EPR spectrum (*29*, *30*).

The EPR results indicate that reduction of hSO with sulfite at low chloride concentrations and at low pH involves the one-electron oxidation of the $Mo^{IV}-OSO_3$ center to a $Mo^{V}-OSO_3$ center (2 → 3A pathway in Scheme 1) to give the *blocked* form. However, the predominant Mo(V) species observed by EPR in the reductive half-reaction may not necessarily be the most catalytically efficient one. The steady-state experiments on SOEs involve a second one-electron oxidation to regenerate the Mo^{VI} form of the enzyme, and the possibility of multiple kinetic pathways for SOEs has been discussed previously (*24*). If the steady-state kinetics experiments at low chloride concentrations and low pH presented here for hSO also involve the *blocked* Mo(V) form (3A of Scheme 1), then a second one-electron oxidation to Mo(VI) could generate a catalytically competent species that could be hydrolyzed to product. Consequently, increasing the chloride concentration can have two competing effects. It can facilitate the dissociation of the product or substrate from Mo(V) state (3A → 3 pathway, Scheme 1) to give the typical *lpH* EPR form, and the amount of this form that is observed depends upon the SOE and the mutation. However, high concentrations of chloride simultaneously decrease the IET rates (*32*) and have an inhibitory effect on the catalytic activity (Table 1). These observations are consistent with a previous extensive microcoulometric study of the effects of anions and pH on the potentials of SO (*33*).

CONCLUSIONS

In contrast to all of the earlier experimental observations (*7*−*10*, *12*, *17*, *19*), in this work we detected, for the first time, the formation of the *blocked* Mo(V) species in *wt* hSO at low pH (pH < 7). The formation of the *blocked* species was traced to the depletion of chloride from the purified enzyme via employment of a large (compared to those used in other laboratories) desalting column. This observation supports the formation of the $Mo-OSO_3$ center as the first step of the catalytic cycle of SO (Scheme 1). Adding NaCl to the *wt* hSO samples where the *blocked* species was formed results in hydrolysis of the product, sulfate, from the Mo active center and the formation of the usual *lpH* species. Similar experiments on several mutant forms of hSO have shown that the formation of the *lpH* species upon addition of Cl^- is mutation-dependent, and the observation of an irreversible *blocked* species for the R160Q mutant of hSO supports the earlier hypothesis for the lethality of this mutation (*16*). Steady-state assays as a function of pH and chloride concentration show that k_{cat} for *wt* hSO decreases with an increase in chloride concentration, but this effect is much smaller at high pH. The combined EPR and kinetic data presented here are

a further indication that the results of specific active site mutations on the chemical and spectroscopic properties of SOEs reflect a subtle interplay of inner- and outer-sphere effects among anions in the media, nearby amino acid side chains, and solvent molecules.

ACKNOWLEDGMENT

We are indebted to Professor K. V. Rajagopalan for providing the pTG918 plasmid containing the hSO gene for preparing recombinant human sulfite oxidase and the protocols for purifying the enzyme. We are grateful to Professor F. Ann Walker for the use of equipment. We thank Dr. Eric L. Klein for preparing the ^{33}S-labeled sulfite and Professor G. Tollin and Dr. A. Raitsimring for helpful discussions. Samples of At-SO and SDH were from previous collaborations (refs *15* and *24*, respectively).

SUPPORTING INFORMATION AVAILABLE

List of mutants, HYSCORE spectra of *wt* hSO enriched with ^{33}S-enriched sulfite at pH 5.8, and kinetic analysis plots for the determination of the binding constant for Cl^-. This material is available free of charge via the Internet at http://pubs.acs.org.

REFERENCES

1. Rajagopalan, K. V. (1980) in Molybdenum and Molybdenum Containing Enzymes (Coughlan, M., Ed.) pp 243−272, Pergamon Press, New York.
2. Johnson, J. L., Rajagopalan, K. V., Renier, W. O., Van der Burgt, I., and Ruitenbeek, W. (2002) Isolated Sulfite Oxidase Deficiency: Mutation Analysis and DNA-Based Prenatal Diagnosis. *Prenatal Diagn. 22*, 433–436.
3. Dublin, A. B., Hald, J. K., and Wootton-Gorges, S. L. (2002) Isolated Sulfite Oxidase Deficiency: MR Imaging Features. *Am. J. Neuroradiol. 23*, 484–485.
4. Karakas, E., Wilson, H. L., Graf, T. N., Xiang, S., Jaramillo-Buswuets, S., Rajagopalan, K. V., and Kisker, C. (2005) Structural Insights into Sulfite Oxidase Deficiency. *J. Biol. Chem. 280*, 33506–33515.
5. Kisker, C., Schindelin, H., Pacheco, A., Wehbi, W., Garrett, R. M., Rajagopalan, K. V., Enemark, J. H., and Rees, D. C. (1997) Molecular Basis of Sulfite Oxidase Deficiency from the Structure of Sulfite Oxidase. *Cell 91*, 973–983.
6. Hille, R. (1996) The Mononuclear Molybdenum Enzymes. *Chem. Rev. 96*, 2757–2816.
7. Cohen, H. J., Fridovich, I., and Rajagopalan, K. V. (1971) Hepatic Sulfite Oxidase: A Functional Role for Molybdenum. *J. Biol. Chem. 246*, 374–382.
8. Kessler, D. L., and Rajagopalan, K. V. (1972) Purification and Properties of Sulfite Oxidase from Chicken Liver. *J. Biol. Chem. 247*, 6566–6573.
9. George, G. N., Garrett, R. M., Graf, T., Prince, R. C., and Rajagopalan, K. V. (1998) Interaction of Arsenate with the Molybdenum Site of Sulfite Oxidase. *J. Am. Chem. Soc. 120*, 4522–4523.
10. Lamy, M. T., Gutteridge, S., and Bray, R. C. (1980) Electron-Paramagnetic-Resonance Parameters of Molybdenum(V) in Sulphite Oxidase from Chicken Liver. *Biochem. J. 185*, 397–403.
11. Gutteridge, S., Lamy, M. T., and Bray, R. C. (1980) The Nature of the Phosphate Inhibitor Complex of Sulphite Oxidase from Electron-Paramagnetic-Resonance Studies using Oxygen-17. *Biochem. J. 191*, 285–288.
12. Bray, R. C., Gutteridge, M. T., Lamy, M. T., and Wilkinson, T. (1983) Equilibria Amongst Different Molybdenum(V)-Containing Species from Sulphite Oxidase. Evidence for a Halide Ligand of Molybdenum in the Low-pH Species. *Biochem. J. 211*, 227–236.
13. Enemark, J. H., Astashkin, A. V., and Raitsimring, A. M. (2010) High Resolution EPR Spectroscopy of Mo-Enzymes. Sulfite Oxidases: Structural and Functional Implications. In Biological Magnetic Resonance. Volume 29. Metals in Biology: Applications of High Resolution EPR to Metalloenzymes (Hanson, G. R., and Berliner, L. J., Eds.) pp 121−168, Springer, Berlin.
14. Enemark, J. H., Astashkin, A. V., and Raitsimring, A. M. (2006) Investigation of the Coordination Structures of the Molybdenum(V) Sites of Sulfite Oxidizing Enzymes by Pulsed EPR Spectroscopy. *Dalton Trans.* 3501–3514.
15. Astashkin, A. V., Johnson-Winters, K., Klein, E. L., Byrne, R. S., Hille, R., Raitsimring, A. M., and Enemark, J. H. (2007) Direct Demonstration of the Presence of Coordinated Sulfate in the Reaction Pathway of *Arabidopsis thaliana* Sulfite Oxidase using ^{33}S Labeling and ESEEM Spectroscopy. *J. Am. Chem. Soc. 129*, 14800–14810.
16. Astashkin, A. V., Johnson-Winters, K., Klein, E. L., Feng, C., Wilson, H. L., Rajagopalan, K. V., Raitsimring, A. M., and Enemark, J. H. (2008) Structural Studies of the Molybdenum Center of the Pathogenic R160Q Mutant of Human Sulfite Oxidase by Pulsed EPR Spectroscopy and ^{17}O and ^{33}S Labeling. *J. Am. Chem. Soc. 130*, 8471–8480.
17. Klein, E. L., Astashkin, A. V., Ganyushin, D., Riplinger, C., Johnson-Winters, K., Neese, F., and Enemark, J. H. (2009) Direct Detection and Characterization of Chloride in the Active Site of the Low-pH Form of Sulfite Oxidase using Electron Spin Echo Envelope Modulation Spectroscopy, Isotopic Labeling, and Density Functional Theory Calculations. *Inorg. Chem. 48*, 4743–4752.
18. Feng, C., Wilson, H. L., Hurley, J. K., Hazzard, J. T., Tollin, G., Rajagopalan, K. V., and Enemark, J. H. (2003) Essential Role of Conserved Arginine 160 in Intramolecular Electron Transfer in Human Sulfite Oxidase. *Biochemistry 42*, 12235–12242.
19. Doonan, C. J., Wilson, H. L., Rajagopalan, K. V., Garrett, R. M., Bennett, B., Prince, R. C., and George, G. N. (2008) Modified Active Site Coordination in a Clinical Mutant of Sulfite Oxidase. *J. Am. Chem. Soc. 130*, 6298–6298.
20. Temple, C. A., Graf, T. N., and Rajagopalan, K. V. (2000) Optimization of Expression of Human Sulfite Oxidase and its Molybdenum Domain. *Arch. Biochem. Biophys. 383*, 281–287.
21. George, G. N., Garrett, R. M., Prince, R. C., and Rajagopalan, K. V. (1996) The Molybdenum Site of Sulfite Oxidase: A Comparison of Wild-Type and the Cysteine 207 to Serine Mutant using X-Ray Absorption Spectroscopy. *J. Am. Chem. Soc. 118*, 8588–8592.
22. Astashkin, A. V., Enemark, J. H., and Raitsimring, A. (2006) 26.5−40 GHz K_a-Band Pulsed EPR Spectrometer. *Concepts Magn. Reson., Part B 29B*, 125–136.
23. Rapson, T. D., Astashkin, A. V., Johnson-Winters, K., Bernhardt, K. V., Kappler, U., Raitsimring, A. M., and Enemark, J. H. (2010) Pulsed EPR Investigations of the Mo(V) Centers of the R55Q and R55M Variants of Sulfite Dehydrogenase from *Starkeya novella*. *J. Biol. Inorg. Chem. 15*, 505–514.
24. Emesh, S., Rapson, T. D., Rajapakshe, A., Kappler, U., Bernhardt, P. V., Tollin, G., and Enemark, J. H. (2009) Intramolecular Electron Transfer in Sulfite-Oxidizing Enzymes: Elucidating the Role of a Conserved Active Site Arginine. *Biochemistry 48*, 2156–2163.
25. Morton, J. R., and Preston, K. F. (1978) Atomic Parameters for Paramagnetic Resonance Data. *J. Magn. Reson. 30*, 577–582.
26. Pacheco, A., Basu, P., Borbat, P., Raitsimring, A. M., and Enemark, J. H. (1996) Multifrequency ESEEM Spectroscopy of Sulfite Oxidase in Phosphate Buffer: Direct Evidence for Coordinated Phosphate. *Inorg. Chem. 35*, 7001–7008.
27. Bray, R. C., Lamy, M. T., and Gutteridge, S. W. T. (1982) Evidence from Electron-Paramagnetic-Resonance Spectroscopy for a Complex of Sulfite Ions with the Molybdenum Centre of Sulfite Oxidase. *Biochem. J. 201*, 241–243.
28. Enemark, J. H., Raitsimring, A. M., Astashkin, A. V., and Klein, E. L. (2010) Implications for the Mechanism of Sulfite Oxidizing Enzymes from Pulsed EPR Spectroscopy and DFT Calculations for "Difficult" Nuclei. *Faraday Discuss.* (in press).
29. Astashkin, A. V., Mader, M. L., Enemark, J. H., Pacheco, A., and Raitsimring, A. M. (2000) Direct Detection of the Proton-Containing Group Coordinated to Mo(V) in the High-pH Form of Chicken Liver Sulfite Oxidase by Refocused Primary ESEEM Spectroscopy: Structural and Mechanistic Implications. *J. Am. Chem. Soc. 122*, 5294–5302.
30. Astashkin, A. V., Klein, E. L., Ganyushin, D., Johnson-Winters, K., Neese, F., Kappler, U., and Enemark, J. H. (2009) Exchangeable Oxygens in the Vicinity of the Molybdenum Center of the High-pH Form of Sulfite Oxidase and Sulfite Dehydrogenase. *Phys. Chem. Chem. Phys. 11*, 6733–6742.
31. Sullivan, E. P., Hazzard, J. T., Tollin, G., and Enemark, J. H. (1993) Electron Transfer in Sulfite Oxidase: Effects of pH and Anions on Transient Kinetics. *Biochemistry 32*, 12465–12470.
32. Pacheco, A., Hazzard, J. T., Tollin, G., and Enemark, J. H. (1999) The pH Dependence of Intramolecular Electron Transfer Rates in Sulfite Oxidase at High and Low Anion Concentrations. *J. Biol. Inorg. Chem. 4*, 390–401.
33. Spence, J. T., Kipke, C. A., Enemark, J. H., and Sunde, R. H. (1991) Stoichiometry of Electron Uptake and the Effect of Anions and pH on the Molybdenum and Heme Reduction Potentials of Sulfite Oxidase. *Inorg. Chem. 30*, 3011–3015.